Non-Neoclassical Up/Down Asymmetry of Impurity Emission on Alcator C-Mod

M.L. Reinke, J.E. Rice, I.H. Hutchinson, M. Greenwald, N.T. Howard,
J.W. Hughes, J. Irby, Y. Podpaly, J.L. Terry and A. White
MIT-Plasma Science and Fusion Center
Cambridge, MA, USA

December 7, 2012

Abstract

We demonstrate that existing theories are insufficient to explain up/down asymmetries of argon X-ray emission in Alcator C-Mod Ohmic plasmas. Instead of the poloidal variation, $\tilde{n}_z/\langle n_z \rangle$, being of order the inverse aspect ratio, ϵ, and scaling linearly with $B_t \bar{n}_e / I_p^2$, it is observed over $0.8 < r/a < 1.0$ to be of order unity and exhibits a threshold behavior between $3.5 < B_t \bar{n}_e / I_p < 4.0$ [T10^{20}m^{-3}/MA]. The transition from symmetric to asymmetric impurity distribution is shown to occur at densities just below those that trigger a reversal of the core toroidal rotation direction, thought to be linked to the transition between the linear and saturated Ohmic confinement regimes. A possible drive is discussed by which anomalous radial transport might sustain the impurity density asymmetry as the ratio of the perpendicular to parallel equilibration times, $\tau_{\perp,z}/\tau_{\parallel,z}$, approaches unity. This explanation requires a strong up/down asymmetry in radial flux which, while not observable on C-Mod, has been measured in TEXT and Tore Supra Ohmic plasmas.

1 Introduction

In tokamaks, the density of impurities has been shown to exhibit substantial variations along a flux surface, $n_z(\theta)/\langle n_z\rangle = 1 + \tilde{n}_z/\langle n_z\rangle$ in cases where the main ion and electron species are nominally poloidally symmetric, $n_i(\theta)/\langle n_i\rangle \ll 1$. This poloidal variation is thought to be explained by neoclassical theory by solving the coupled continuity and momentum balance equations along the field for the impurities, main-ions and electrons. Strong in/out asymmetries have been observed in a range of experiments, driven by inertia [1][2] and poloidal electric fields [3][4], while ion-impurity friction can also play a role, leading to both up/down [5][6] and in/out asymmetries [7][8]. Validating the physical models driving the poloidal variation of n_z demonstrates a basic understanding of how parallel equilibrium is established in a tokamak plasma and allows main-ion flows to be inferred from the more routine measurement of impurity flows. Both neoclassical [9] and, more recently, turbulent-driven [10] flux-surface averaged radial impurity transport have been shown to be sensitive to the details of $n_z(\theta)$. Additionally, unaccounted for poloidal impurity variation can lead to systematic error when interpreting measurements from diagnostics with limited coverage of the 2D cross-section [11][12].

This research reports on measurements of flux surface variations of order unity, $\tilde{n}_z/\langle n_z\rangle \sim 1$, in He-like argon line emission in Alcator C-Mod Ohmic plasmas. While an up/down asymmetry in argon X-ray emission has previously been reported on C-Mod [13] using an array of single-chord spectrometers, this research expands those measurements over a substantial portion of C-Mod's Ohmic operating space by exploiting an X-ray imaging crystal spectrometer [14]. Measurements of the poloidal variation are larger than predicted by neoclassical theory and display a threshold-type behavior, rather than scaling linearly with $\bar{n}_e B_t/I_p^2$. Instead, between $3.5 < \bar{n}_e B_T/I_p < 4.0$, the poloidal impurity distribution transitions from nominally flux-surface symmetric state, $\tilde{n}_z/\langle n_z\rangle < 0.1$, for $r/a > 0.8$ to one that is strongly asymmetric, $\tilde{n}_z/\langle n_z\rangle \simeq 1$, as $\bar{n}_e B_T/I_p$ increases. This transition is observed at electron densities near, although systematically lower than, that of the so-called rotation reversal [15][16], shown to occur at the boundary between the linear Ohmic (LOC) and saturated Ohmic confinement (SOC) regimes [17][18].

The prompt change in the up/down asymmetry near the LOC/SOC transition and the observed strong anomalous radial transport at large minor radii is consistent with an explanation that the up/down asymmetry may be caused by a poloidally varying radial particle flux. The argon X-ray emission at 3.3 keV is measured in regions of the plasma with T_e of only a few hundred eV, driven by recombination from Ar^{17+}. To have measurable emission from this process implies that the cross-field transport time scale, $\tau_\perp$, is less than the recombination time, τ_{REC}, to enable Ar^{17+} to be present at $r/a \sim 0.9$ [19]. If the parallel equilibration time of the impurities, $\tau_\parallel$, becomes close to $\tau_\perp$, then anomalous radial transport can influence the parallel force balance. If this radial transport is not uniform on a flux surface then it will result in a poloidal asymmetry, qualitatively similar to how a poloidally varying limiter source has been shown influence the up/down asymmetry in low-Z emission [5][20]. While measurements of such an up/down asymmetry of turbulence are currently not possible at Alcator C-Mod, observations have been made previously on TEXT [21] and Tore-Supra [22] that show not only an up/down asymmetry in n_e fluctuations at large minor radii, but also show this phenomenon reverses sign, up/down goes to down/up, with the reversal of the direction of the current with respect to the toroidal field. This is consistent with present and previously reported

observations [13] of the up/down asymmetry in Ar emission reversing with the ∇B drift direction since Alcator C-Mod must reverse both current and toroidal field directions to maintain the same helicity due to design of plasma facing components. Due to parity arguments, such a reversal of current cannot lead to changes on nearly-up/down symmetric flux surfaces, but edge turbulence induced by poloidally asymmetric boundary conditions has been shown to have an impact in the outer region of the confined plasma [23].

In this paper, Section 2 provides a brief background of the theory and summary of previous observations of up/down impurity asymmetries in tokamak plasmas. Section 3 discusses the experimental and analysis techniques used to measure the up/down asymmetry over a large portion of C-Mod's Ohmic operating space. Section 4 presents the parametric trends in the asymmetry, demonstrating the threshold behavior in $\tilde{n}_z/\langle n_z \rangle$ while Section 5 discusses the possibility of these results as being driven by poloidally varying turbulent radial particle flux.

2 Background

Up/down asymmetries of impurity emission have been observed in many tokamaks using conventional soft x-ray tomography [24][25][26] and bolometry tools [6], or employing poloidally scanning spectrometers [27][20][13]. The impurity emission above the midplane is measured and compared to that below the midplane, where, assuming n_e and T_e are flux functions, the emission ratio will be equivalent to the ratio of impurity density, $n_z(\pi/2)/n_z(3\pi/2)$. The poloidally varying component, normalized to the flux-surface average, is computed from such observations via $\tilde{n}_z/\langle n_z \rangle = 0.5[n_z(\pi/2) - n_z(3\pi/2)]/[n_z(\pi/2) + n_z(3\pi/2)]$. Measurements consistent with neoclassical theory have been observed for carbon, with $\tilde{n}_z/\langle n_z \rangle$ scaling like $n_e B_t/I_p^2$ [5][6]. In other cases where the up/down asymmetry of low ionization states of impurities did not exhibit behaviors consistent with neoclassical predictions, the explanation was that strong poloidally localized impurity sources were likely the cause [20][28]. Recent measurements of up/down asymmetries of molybdenum density in the core, $r/a < 0.8$, of C-Mod plasmas also showed disagreement with neoclassical theory [29], although only small asymmetries, $|\tilde{n}_z/\langle n_z \rangle| < 0.1$, were observed.

The up/down asymmetry of soft x-ray emission from highly-ionized Ar has previously been observed on Alcator C-Mod [13] using a 5-channel von Hamos spectrometer [30], where chords could be scanned poloidally between shots. By repeating discharges, the full poloidal cross-section could be scanned at fixed field, current and density . This was completed for USN and LSN plasmas in both forward and reversed field. The sense of the asymmetry was shown to flip when running C-Mod in reversed field, with emission always higher in the direction opposite the ion ∇B drift direction, independent of the location of the X-point. Again, both current and field directions are changed simultaneously in C-Mod in order to maintain the same helicity.

Parallel neoclassical impurity transport theory in the Pfirsch-Schlüter (PS) [31], plateau (PLAT) [32] and banana (BAN) [9] regimes predict an up/down asymmetry that is driven by ion-impurity friction. In steady-state, source-free plasmas, $\nabla \cdot (n\mathbf{v}) = 0$ leads to an ion species having a flow velocity of

$$\mathbf{v}_a = \frac{K_a(\psi)}{n_a(\psi,\theta)}\mathbf{B} - \left(\frac{\partial \Phi}{\partial \psi} + \frac{T_a}{Z_a e n_a(\psi,\theta)}\frac{\partial n_a(\psi,\theta)}{\partial \psi}\right) R\hat{\phi} \tag{1}$$

where n_a is the radially and poloidally varying particle density, T_a is the flux-surface symmetric temperature, Φ is the electrostatic potential and K_a is a flux-function that is found by solving the parallel momentum balance equation using a periodic boundary condition, $n_a(\psi, 0) = n_a(\psi, 2\pi)$. Even in the absence of any mean parallel flow, $K_a = 0$, the difference in diamagnetic flow, due to the $1/Z_a$ dependence is sufficient to drive asymmetries from ion-impurity friction. The up/down asymmetry in the circular, low-inverse aspect ratio approximation takes the form, $\tilde{n}_z/\langle n_z \rangle \simeq 2\epsilon g$, where g is collisionality dependent, with

$$g_{PS} = -\frac{m_i Z^2 I}{e\tau_{ii}\langle \mathbf{B}\cdot\nabla\theta\rangle}\frac{1}{n_i}\frac{\partial n_i}{\partial\psi} \tag{2}$$

$$g_{BAN} = -\frac{m_i Z^2 I}{e\tau_{ii}\langle \mathbf{B}\cdot\nabla\theta\rangle}\left(\frac{1}{n_i}\frac{\partial n_i}{\partial\psi} - 0.5\frac{1}{T_i}\frac{\partial T_i}{\partial\psi}\right) \tag{3}$$

$$g_{PLAT} = -\frac{m_i Z^2 I}{e\tau_{ii}\langle \mathbf{B}\cdot\nabla\theta\rangle}\frac{1}{p_i}\frac{\partial p_i}{\partial\psi} \tag{4}$$

where the subscript i refers to the main-ions, assumed to be hydrogenic, and I refers to the toroidal field as per $\mathbf{B} = I(\psi)\nabla\phi + \nabla\psi\times\nabla\phi$. While the response to the kinetic profile gradient scale length varies, all profiles have the same leading factor which scales approximately as $n_e B_t/I_p^2$ for fixed impurity species. Additionally, as g becomes large when the ion-impurity friction increases, theory predicts a transition to an in/out asymmetry, with the up/down asymmetry scaling like $\tilde{n}_z/\langle n_z\rangle \simeq 2\epsilon g/(1+g^2)$. As g becomes large, this results in the maximum up/down asymmetry of the size of the inverse aspect ratio, $\tilde{n}_z/\langle n_z\rangle < \varepsilon$, less than 0.3 near the boundary of C-Mod.

3 Description of Experiment and Analysis Techniques

In order to empirically examine the dependencies of the up/down asymmetry, a substantial portion of C-Mod's Ohmic operating space is investigated. At fixed plasma shape, the electron density is scanned during the current and field flattop, with I_p and B_t adjusted shot-to-shot. Figure 1 shows the range of $(\bar{n}_e, I_p)$ covered at each of three toroidal fields, $B_t = 3.3$, 5.4 and 7.5 T.

The up/down asymmetry of the $1s^2$-1s2s line emission in He-like Ar is observed using an x-ray imaging crystal spectroscopy (XICS) [14][11]. In Figure 2, the magnetic geometry is displayed along with the lines of sight of the imaging x-ray crystal spectrometer. A mask was placed over the crystal, reducing its effective size by $> 50\%$, down from its normal size of 6.4×2.7 cm. While this reduces throughput, the spatial resolution is enhanced, enabling detailed emissivity profiles to be found at larger minor radii. The low-field side viewing geometry of the spectrometer makes this system insensitive to in/out asymmetries [11], but these have been demonstrated to be small, $\tilde{n}_z/\langle n_z\rangle \simeq 0.1$, in Ohmic plasmas [29]. The time and spatial resolution of XICS enables as much data to be collected per time slice as was done during an entire day of operations using the von Hamos system in [30].

The spectrometer also measures the ion temperature and rotation profiles over the entire plasma cross-section. Electron temperature and density profiles are measured using Thomson scattering with additional density measurements provided by interferometry, and additional T_e data at higher

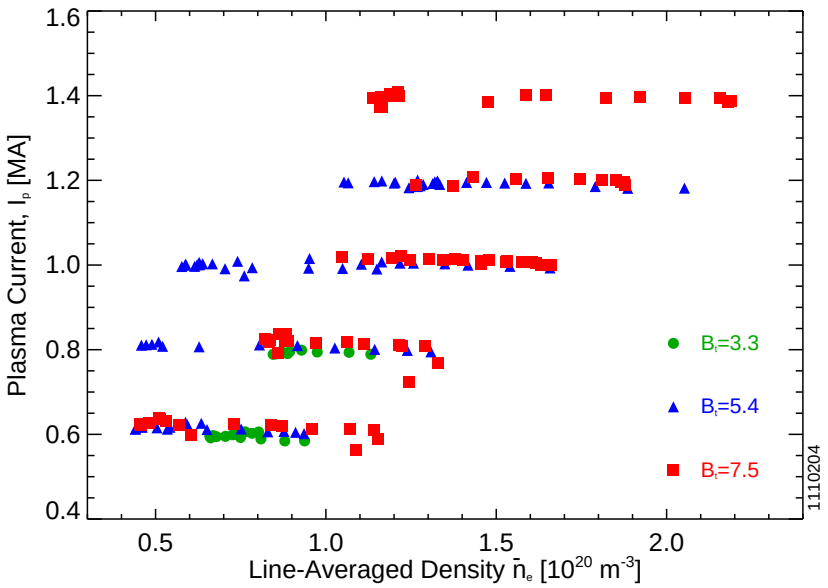

Figure 1: The I_p, B_t and $\bar{n}_e$ operating space used in analyzing trends in the up/down Ar asymmetry

B_t provided by electron cyclotron emission [33]. While not shown, the photodiode-based soft x-ray tomography diagnostic shows qualitatively similar up/down asymmetries as the crystal spectrometer in cases where argon dominates the soft x-ray power loss.

3.1 Origin of the Ar Line Emission

The $1s^2$-1s2s transition in He-like Ar, the forbidden line or the z-line in Gabriel notation [34], is used for these investigations. Although the 1s2s level of He-like ions is considered a metastable state, the transition probability is $\sim 10^6$ s^{-1}, allowing it still to be considered a probe of local plasma conditions. As discussed in prior work [13], this excited state can be populated by three different mechanisms, excitation from the ground state of Ar^{16+}, inner-shell ionization of Ar^{15+}, and recombination from Ar^{17+}. Both excitation and inner-shell ionization occur at high electron temperatures, $T_e \sim 1$ keV, while recombination from H-like Ar dominates at low temperatures. Figure 3 shows the T_e dependent $\langle \sigma v \rangle$ from all three charge states computed using the Flexible Atomic Code (FAC) [35].

Line-integrated spectra from a discharge that is nominally up/down symmetric are shown in Figure 4, demonstrating that not only the brightness, but also the line-width, and thus ion-temperature, is up/down symmetric. For the core view, 4a, the width of the z-line at $\lambda \simeq 3.994$Å is much wider than either of the views at $r/a \sim 0.9$ shown in 4b. Additionally, the $n = 2$ satellite transitions between 3.980 Å $< \lambda <$ 3.992 Å that are populated by inner-shell ionization and dielectronic recombination, are only seen in the core plasma. Both of these observations are typical of this data set as a whole. As discussed in [13], the change in the relative amplitudes of the resonance (w) and forbidden line indicate that direct excitation is strongly suppressed leaving recombination as the mechanism for populating the 1s2s state at $r/a \simeq 0.9$.

Figure 5 illustrates how recombination-driven X-ray emission can occur in such cold regions of the

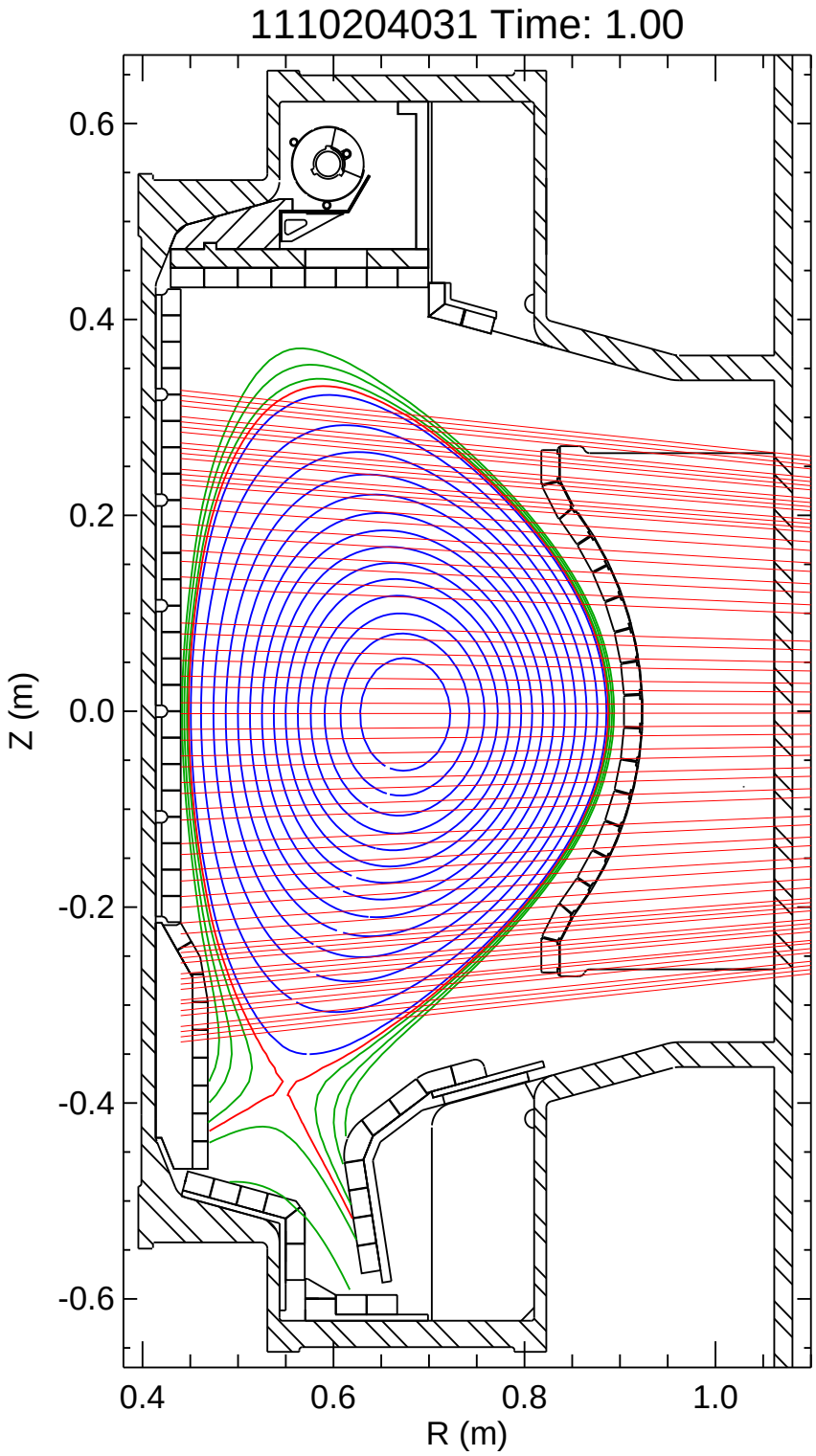

Figure 2: Typical equilibrium used in the parameter scan with the HIREXSR lines of sight included

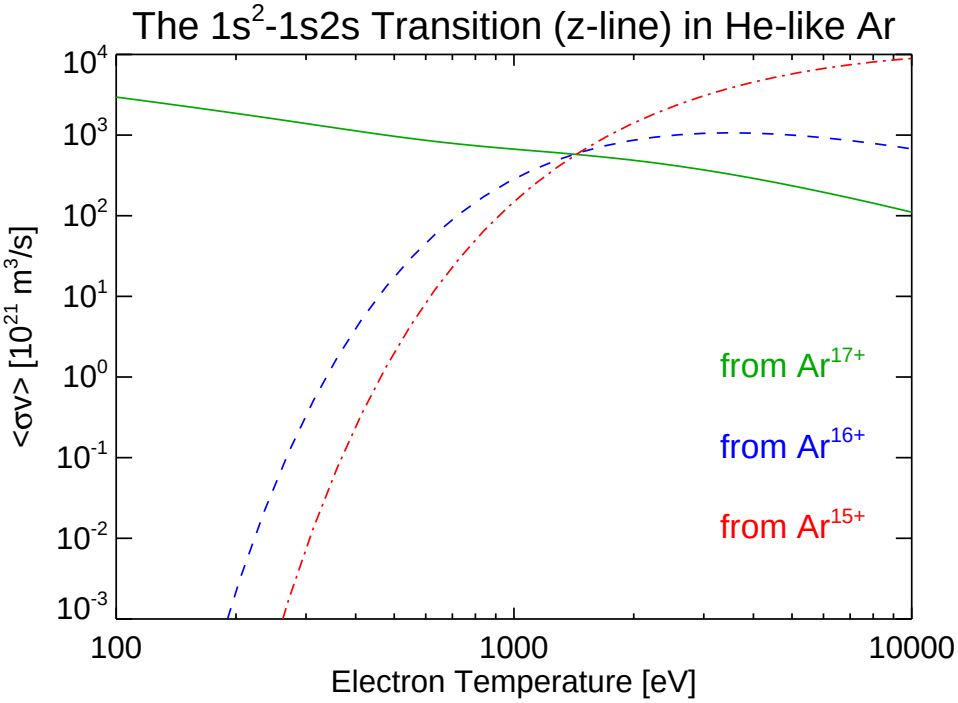

Figure 3: Photon emission coefficients, $\langle \sigma v \rangle$, for the 1s^2-1s2s transition in He-like Ar

plasma when there is strong radial transport. In the core of the plasma, a thermalized Ar^{16+} ion (red) is ionized to become a hot Ar^{17+} ion. It cools as it is transported radially outward, likely by diffusion since it remains in thermal equilibrium with the local plasma (purple), until it becomes a cold Ar^{17+} ion near the edge of the plasma (blue). As it moves to the low-T_e plasma, the recombination-rate increases and when it occurs, the 1s2s state is preferentially populated, quickly decaying to the Ar^{16+} ground state. The direct excitation path is very weak in the cold plasma, as is the inner-shell ionization of Ar^{15+}, and thus the ion must cycle back through the core plasma in order to contribute to the observed edge X-ray emission. Note a charge-exchange reaction will also lead to the same process occurring and will be included in discussion in Section 5.

3.2 Example Profiles

Both up/down symmetric and asymmetric profiles are observed over the range of this parameter scan. In Figure 6a, the raw brightness profiles are shown for a case with little asymmetry, while Figure 6b demonstrates a case with a substantial asymmetry, with increased emission for $Z > 0$. This is the direction away from the ion ∇B drift direction and is observed to reverse when the I_p and B_t directions are reversed, but not when the position of the x-point is switched.

These brightness profiles can then be tomographically inverted and the asymmetry determined by assuming that the emissivity has the form,

$$\varepsilon = \varepsilon_0 (\psi) + \varepsilon_1 (\psi) \sin \theta \tag{5}$$

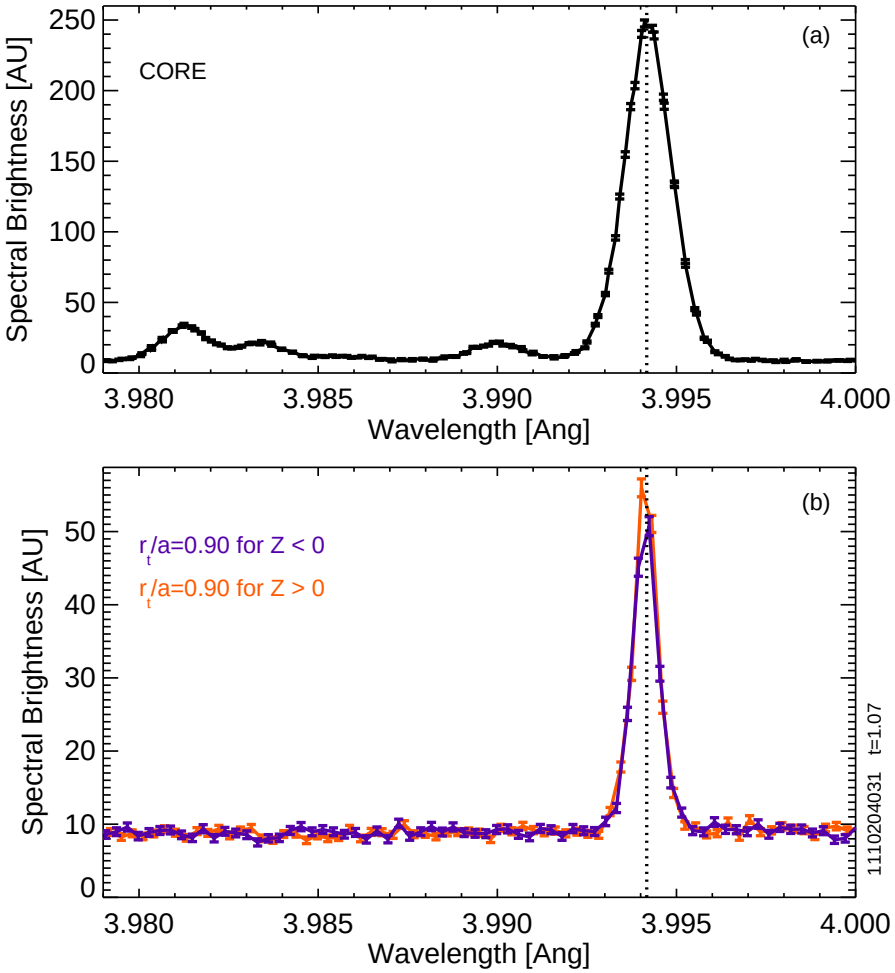

Figure 4: Spectra for the core (a) and chords at $r/a = 0.9$ (b) for the up/down symmetric case shown in Figure 6a

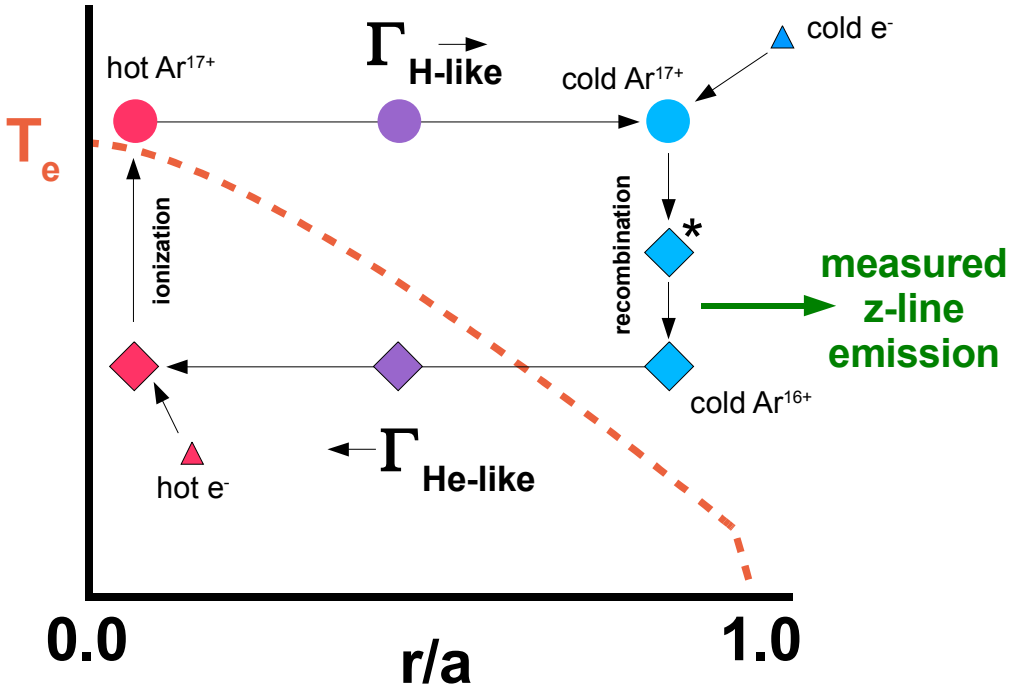

Figure 5: Diagram of how the 1s2s excited state is populated via recombination

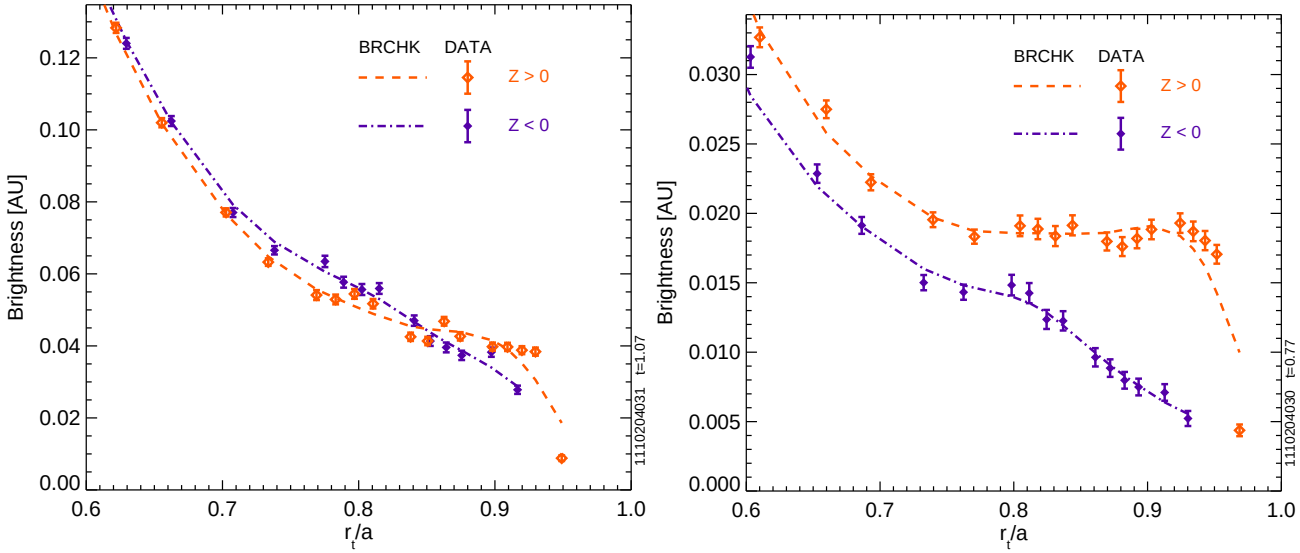

(a) (b)

Figure 6: Brightness profiles showing weak or negligible up/down asymmetry in a 1.0 MA, 5.4 T plasma at $\bar{n}_e \simeq 0.6 \times 10^{20}$ m^{-3} (a) and a strong up/down asymmetry in a 0.6 MA, 5.4 T plasma at $\bar{n}_e \simeq 0.5 \times 10^{20}$ m^{-3} (b)

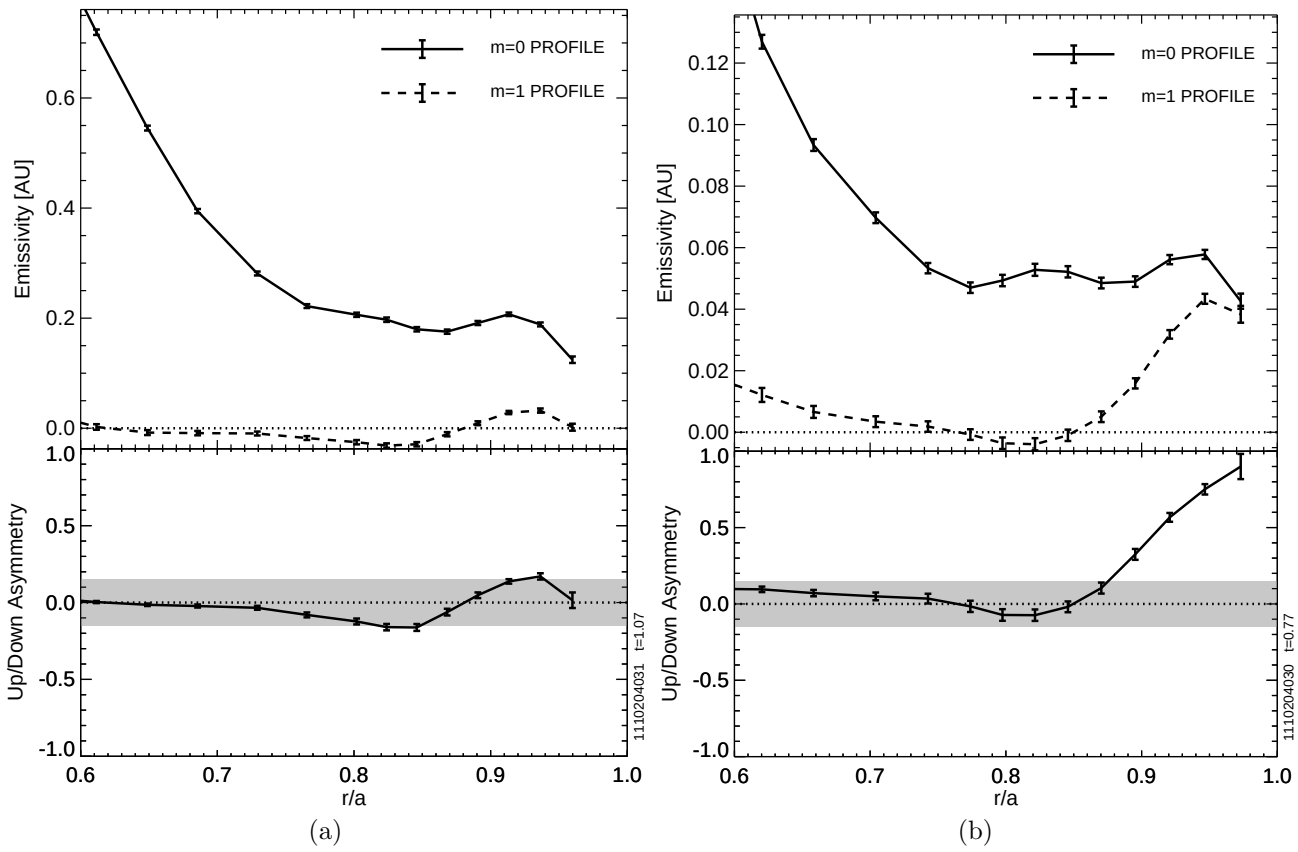

(a) (b)

Figure 7: Emissivity profiles calculated from data shown in Figures 6a 6b, showing a weak (a) and strong (b) up/down asymmetry

Figure 7 shows plots of these $m = 0$ and $m = 1$ components of the emissivity from (5) in the outer half of the plasma for the brightness profiles displayed in Figure 6. If this emission is due to electron impact processes, then $\varepsilon = n_z n_e L(T_e)$. By taking the ratio of $\varepsilon_1/\varepsilon_0$, referred to as the up/down asymmetry, the poloidally varying component of the impurity density is isolated, assuming that electron density and temperature are both flux functions which should be valid on closed field lines in an Ohmic plasma. No asymmetry is observed outside of the $\pm$ 15% flat-field calibration error indicated by the grey shading in Figure 7a. In Figure 7b, the up/down asymmetry is plotted over the same range in minor radius. A transition is observed between a region of little to no poloidal asymmetry for $r/a < 0.85$ to a region of strong variation approaching the separatrix.

4 Parametric Scaling of the Up/Down Asymmetry

The emissivity profiles for multiple time points in 17 discharges are used to determine the scaling of the up/down asymmetry with global plasma parameters over a large portion of C-Mod's Ohmic operating space, as shown in Figure 1. The radial location of $r/a = 0.92$ is used to characterize the edge asymmetry layer, which previously was unable to be reproduced by parallel neoclassical

transport theory [13]. In Figure 8a, the up/down asymmetry data for $B_t = 5.4$ T plasmas are plotted against line-averaged density, $\bar{n}_e$, for various plasma currents. Systematic differences between the different range of currents are reduced when plotting the up/down asymmetry against $\bar{n}_e/I_p$, as shown in Figure 8b. In this plot, the asymmetry is shown to have a threshold type behavior, increasing from near symmetry to a $\tilde{n}_z/\langle n_z \rangle \simeq 0.6$ between $0.6 < \bar{n}_e/I_p < 0.8$ in units of $[10^{20}\mathrm{m}^{-3}/\mathrm{MA}]$. All shots have a minor radius of ~ 0.20 meters, making $\bar{n}_e/I_p = 1.5$ equivalent to a density that is approximately 20% of the Greenwald density limit. The magnitude of the up/down asymmetry at $r/a = 0.92$ is characteristic of the fully developed asymmetric emission layer shown by Figures 6b and 7b.

The same plot is shown in Figure 9, now including data from all toroidal fields. The B_t=3.3 points (green) exhibit a similar type of threshold behavior as the 5.4 T shots (blue), although at a higher value of $\bar{n}_e/I_p$, while the high field shots (red) are nearly all asymmetric. The measured asymmetry is shown to decay back towards zero for larger values of $\bar{n}_e/I_p$, although with relatively large error bars.

As pointed out in TEXTOR research on the He-like Ar $n = 2$ spectrum [36], the charge-exchange (C-X) recombination process can populate the 1s2s state preferentially over the 1s2p states. In most C-Mod plasmas, the high density leads to a short neutral decay length and neutral fractions can remain below 10^{-4}. As Ohmic plasmas are fueled by main-chamber gas puffing and recycling, at high densities the neutral pressure can increase to $\sim$0.5 mTorr, increasing the contribution of forbidden line emission due to C-X. In Figure 10, the asymmetry is plotted against neutral pressure, p_{neut}, measured by a ratiomatic gauge at the outboard midplane vessel wall at $R = 1.04$ m, and the decay of the asymmetry at large $\bar{n}_e/I_p$ is shown to occur for $p_{neut} > 0.2$ mTorr. In this case, the up/down argon density asymmetry could begin to be driven by C-X if the neutral density is not poloidally symmetric. Prior measurements of both Lyman-α emissivity and neutral pressure show the neutral density is higher in the direction of the X-point [37]. Thus, the data in Figure 10 suggest charge-exchange recombination adjusts the argon emission back towards symmetry, in the direction of the X-point, as the neutral pressure increases.

In Figure 11, the asymmetry is plotted against $B_t\bar{n}_e/I_p$, but restricting the data set for values of main-chamber pressure below $p_{neut} = 0.2$ mTorr. This is shown to unify the data for all toroidal field strengths and illustrates the up/down asymmetry increasing from near symmetry when $3 < B_t\bar{n}_e/I_p < 5$ $[\mathrm{T}10^{20}\mathrm{m}^{-3}/\mathrm{MA}]$, saturating at a level of $\tilde{n}/\langle n_z \rangle \sim 0.6$.

The change in the asymmetry as the density is increased at fixed field and current is observed dynamically as well. In Figure 12, the time evolution of the asymmetry (d) is plotted for a discharge where $\bar{n}_e$ (a) increases from 0.6 to $1.2{\times}10^{20}$ m^{-3}. At $r/a = 0.82$, the asymmetry remains largely unchanged as the density is increased while at $r/a = 0.92$, the asymmetry quickly increases and asymptotes after only a $\sim$20% rise in density. In Figure 12c, the core rotation frequency is measured, also using the X-ray spectrometer, which demonstrates that just after the asymmetric emission layer forms, the direction of the core-rotation reverses. This change in rotation has been linked to the transition from the Linear Ohmic Confinement (LOC) to Saturated Ohmic Confinement (SOC) operating regime and recent studies on C-Mod have further demonstrated the correlation between the up/down asymmetry and the rotation reversal [38]. The development of the asymmetric argon density layer has been shown to occur systematically at a density just below that where the rotation

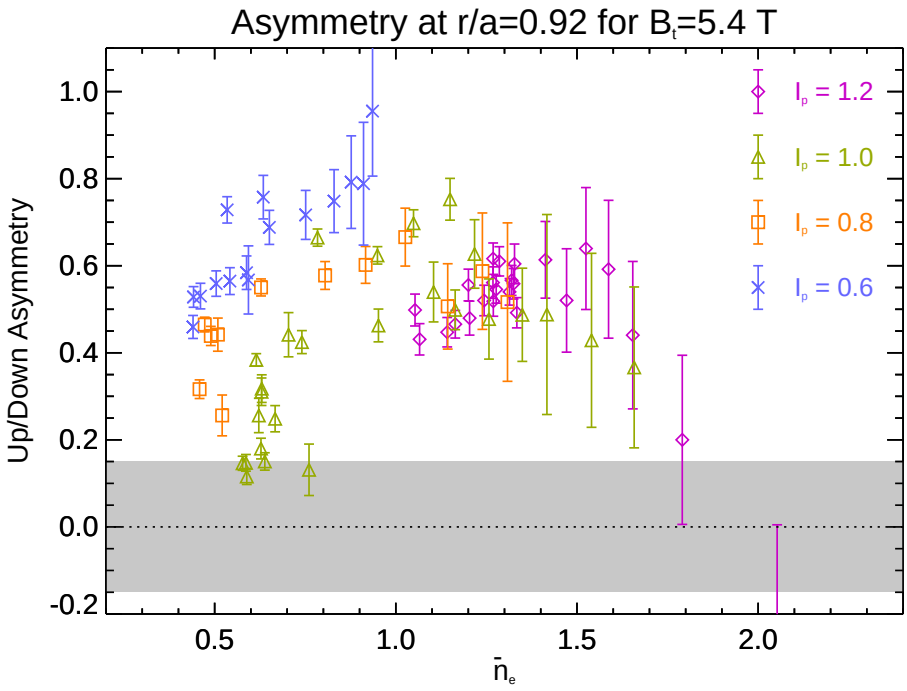

(a)

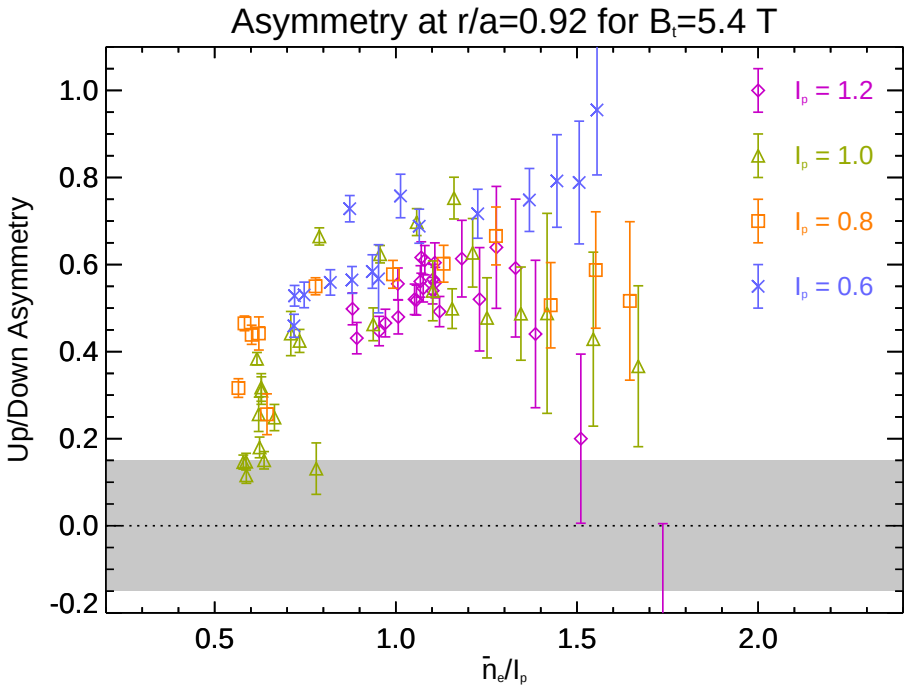

(b)

Figure 8: At fixed toroidal field, up/down asymmetry scales differently with density [10^{20}m^{-3}] at different currents (a), and shows much better scaling when plotted against $\bar{n}_e/I_p$ [10^{20}m^{-3}/MA](b)

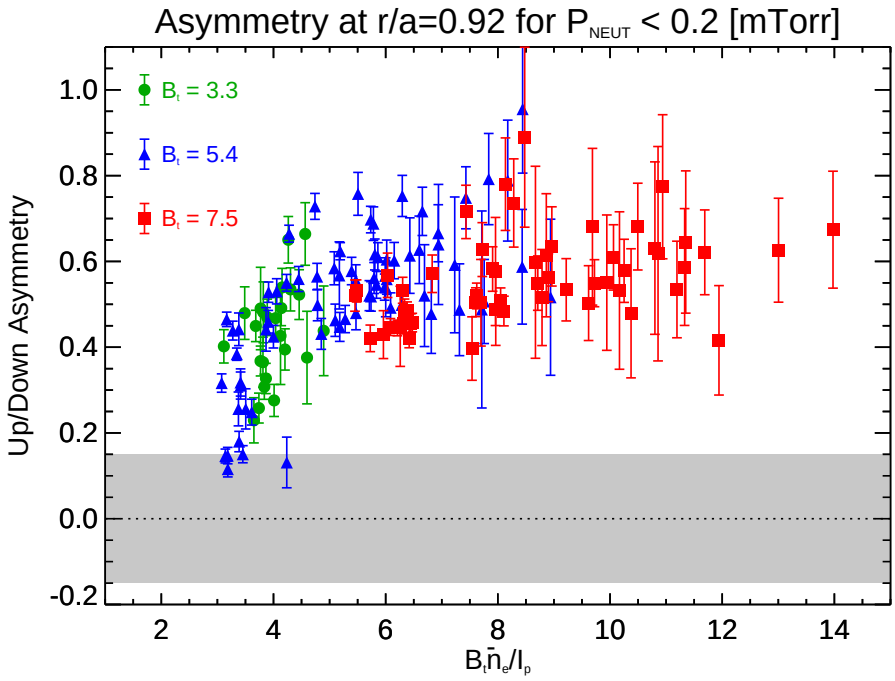

Figure 9: Up/down asymmetry plotted against $\bar{n}_e/I_p$ [$10^{20}\mathrm{m}^{-3}/\mathrm{MA}$] for multiple toroidal fields

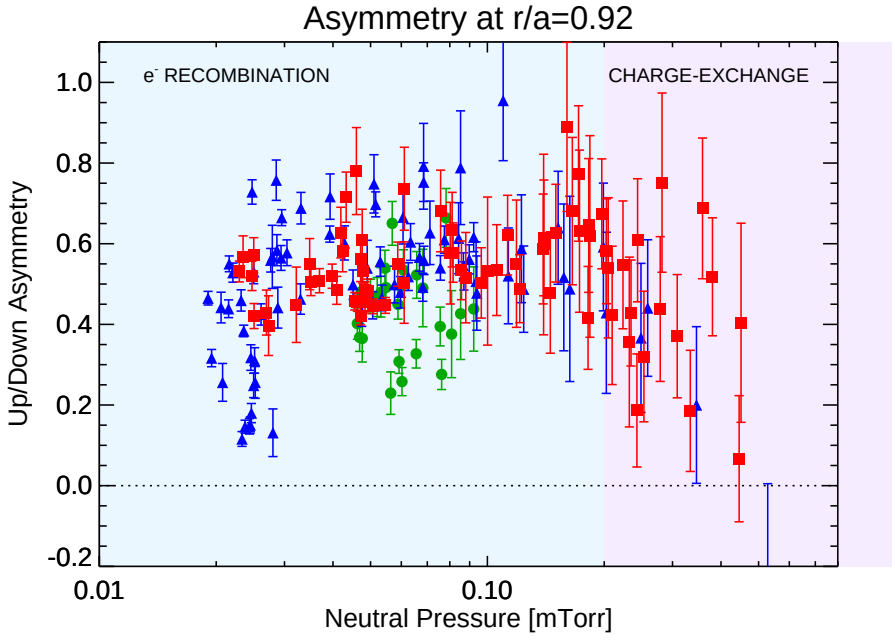

Figure 10: The up/down symmetry is decreased at large values of main-chamber neutral pressure, p_{neut}

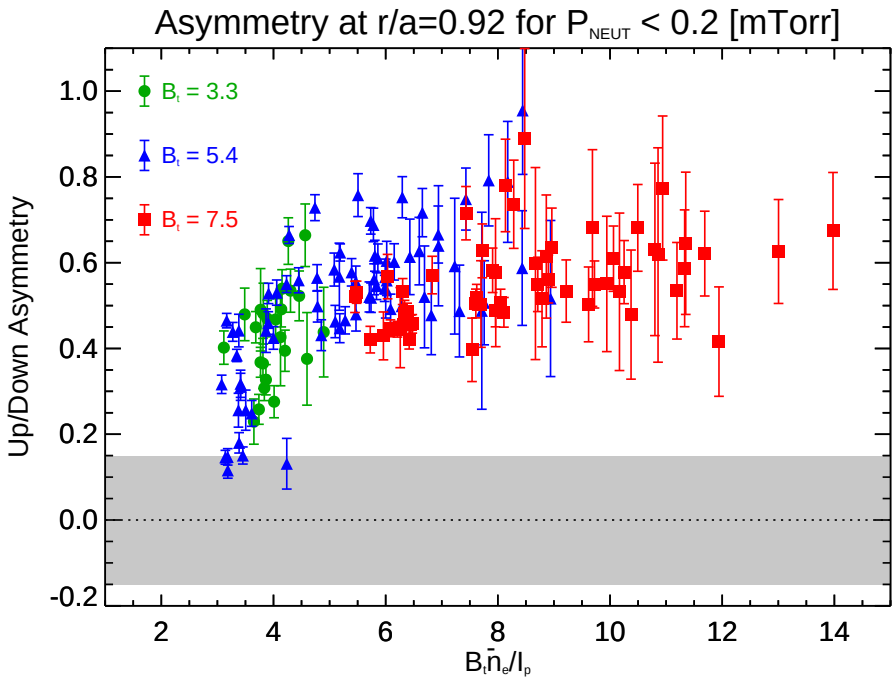

Figure 11: Up/down asymmetry plotted against $B_t\bar{n}_e/I_p$ [T10^{20}m^{-3}/MA] for time points where $p_{neut} \leq 0.2$ mTorr

changes.

5 A Turbulence Driven Asymmetry

The previous section qualitatively shows that the strong up/down asymmetry in Ar^{17+} density is unlikely to be explained by neoclassical parallel impurity transport theory. Poloidal variation, $\tilde{n}_z/\langle n_z \rangle$ of order unity is regularly observed while neoclassical theory predicts the maximum to be of order a/R_o. Rather than show a smooth increase with $B_T\bar{n}_e/I_p^2$, as indicated by theory [5][9], the asymmetry at $r/a = 0.92$ exhibits a transition between a weak and strong asymmetry at $B_t\bar{n}_e/I_p \sim 4$. While the qualitative characteristics of this asymmetry are similar to up/down asymmetries explored on other tokamaks, there is an important difference in the origin of the line emission for the C-Mod case. Earlier experiments viewed resonance transitions from low-Z impurity ions [5] or broadband emission using bolometry [6]. As discussed earlier, the Ar^{16+} 1s2s excited state is populated by recombination from Ar^{17+} ions at low electron temperatures. These ions must be transported from the core of the plasma as shown in Figure 5, and so the very existence of measurable emission at large minor radii is tied to anomalous impurity transport. If this turbulent transport is shown to be strong enough to make $\tau_\perp < \tau_\parallel$, and the radial flux is up/down asymmetric, then the density asymmetry could be sustained by plasma turbulence. The Doppler broadening of the z-line shown in Figure 4 demonstrates that the temperature of the impurity is closer to that of the local electron temperature, rather than the ion temperature in the core where the Ar^{17+} ion was created. This

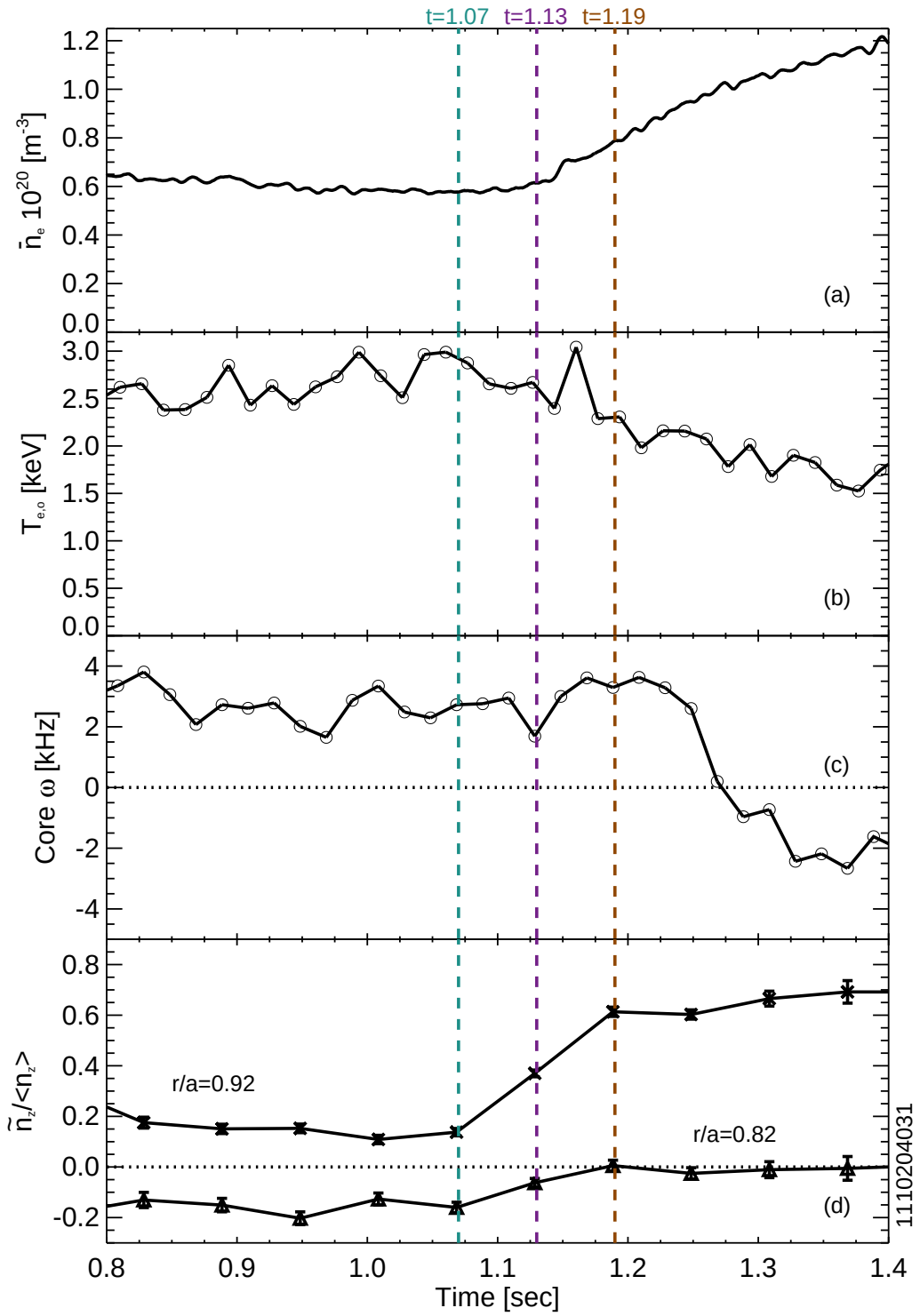

Figure 12: Time history demonstrating the prompt change in the up/down asymmetry due to a small change in $\bar{n}_e$ is linked to the change in the direction of the core rotation

would rule out ballistic transport, indicating that the H-like argon ion has had time to collisionally equilibrate with the background plasma, and the radial transport is diffusive or convective.

While measurement of any poloidal inhomogeneity in the turbulence was not possible for these C-Mod plasmas, up/down asymmetries in fluctuations have previously been observed in Ohmic plasmas on TEXT [21] and Tore-Supra [22]. Changing the current direction has been shown to reverse observed up/down asymmetries in n_e fluctuation amplitude in laser scattering experiments on TEXT, and the fluctuation asymmetry is localized to the spatial region $0.8 < r/a < 1.0$. Tore-Supra used a movable, poloidally and toroidally localized limiter to demonstrate the connection between an observed up/down asymmetry in edge n_e fluctuations to a modification in the plasma boundary [23]. The argon up-down asymmetry reverses direction when the toroidal field direction is reversed (thus reversing the ion ∇B drift direction), as has been observed previously [13]. This behavior is consistent with an internal plasma physics cause of the asymmetry (such as neoclassical transport) rather than machine asymmetry (e.g. localized limiters or gas sources). However, Alcator C-Mod is designed to be run with fixed helicity and must reverse the direction of the plasma current along with the toroidal field. This configuration change therefore cannot distinguish experimentally between current reversal and field reversal. If the mid-Z up/down impurity asymmetry can be observed on a device which can reverse I_p and B_t independently, a clear test of any link between these two phenomenon can be explored.

Another qualitative indication of the asymmetry being linked to anomalous radial transport is the correlation of its onset with the rotation reversal phenomenon. This has been linked to transition between the linear Ohmic confinement regime (LOC) and the saturated Ohmic confinement regime (SOC) thought also to be a changeover between trapped electron mode (TEM) and ion temperature gradient (ITG) dominated turbulence [17][18]. In this paradigm, for the up/down asymmetry to be driven by poloidally asymmetric radial particle flux, TEM turbulence would need to be up/down symmetric, while ITG is strongly up/down asymmetric. Alternatively, a change in zonal flows [39] across the TEM/ITG transition could impact the balance between parallel and perpendicular equilibration as discussed below.

In order for the up/down asymmetry to be turbulence-driven, the anomalous radial transport must be sufficiently strong to interfere with the parallel impurity equilibrium, $\tau_\perp \sim \tau_\parallel$. In C-Mod the poloidal connection length is ~ 1 meter and observations of poloidal rotation are limited to < 2 km/s by the X-ray spectrometer. This indicates that $\tau_\parallel$ is of order a millisecond. Since the high-Z impurities are always in the Pfirsh-Schlüter regime in these plasmas, $\tau_\parallel \neq L_\parallel / v_{th,z}$ but instead must be collisionally diffusive,

$$\tau_\parallel \simeq \frac{2\sqrt{\pi}}{4\tau_{zi}} \left(\frac{qR_o}{v_{th,z}} \right)^2 \tag{6}$$

or be mixed by the mean poloidal flow, $\tau_\parallel > L_\theta / v_\theta$. Here, $v_{th,z} = \sqrt{2T_z/m_z}$ and

$$\tau_{zi} = \frac{12\pi^{3/2}}{\sqrt{2}} \frac{Z_z^2 \sqrt{m_z} T_i^{3/2} \epsilon_0^2}{n_i Z_i^2 e^4 \ln \Lambda} \tag{7}$$

is taken from [40]. At $n_i = 1.0 \times 10^{20}$ m^{-3}, $T_i = 400$eV and $q = 4$, this leads to a very slow diffusive $\tau_\parallel$ of approximately 40 ms. It his here where zonal flows, presenting as $m = 0$ fluctuations in v_θ

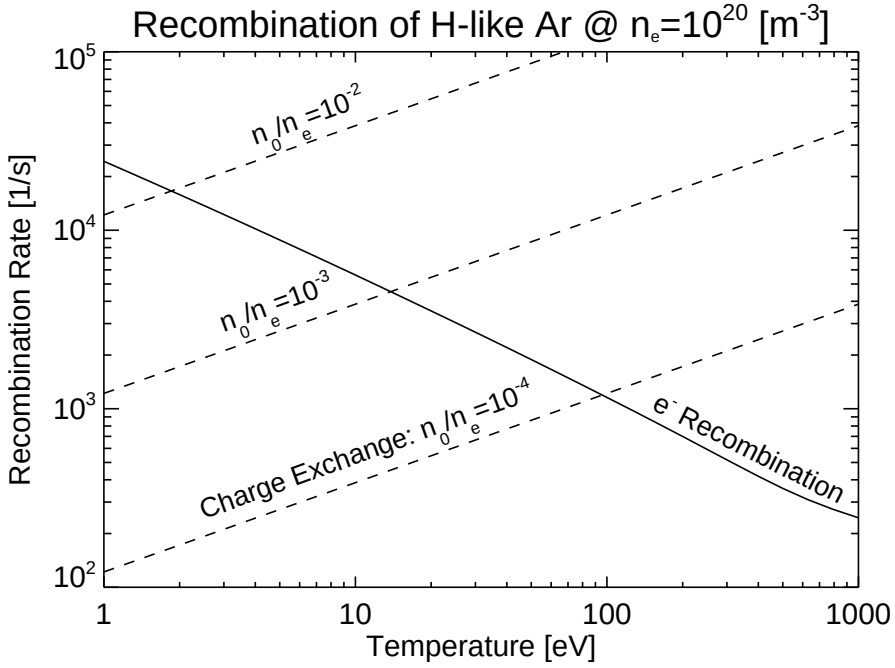

Figure 13: Recombination rates at $n_e = 10^{20}$ m^{-3} for H-like argon due to electron impact (solid) and charge-exchange processes (dashed)

[39], could impact the impurity asymmetry by enhancing poloidal redistribution. Similarly, geodesic acoustic modes (GAMs) have been observed to have an $m = 1$ up/down variation in the density fluctuations [41] and could be enhancing the poloidally asymmetric radial transport to regions where neoclassical parallel transport is too slow. In other tokamaks, GAMs have been localized to the near edge region, $r/a > 0.8$, where the argon density asymmetry is observed for C-Mod [42][43]. While the effect of non-trace impurities has been included in zonal flow [44] and GAM studies [45][46], this physics has not yet been included when determining the steady-state poloidal impurity density variation.

The flux-surface averaged emissivity profiles shown earlier allow an estimation of the perpendicular transport time. Appendix A describes the derivation of a simplified continuity equation for H-like Ar that should be valid at large minor radii where the asymmetry is observed. In order for the emissivity profile to transition from peaked to flat as shown in Figure 7, the radial transport timescale, $\tau_\perp$, would have to become less than the recombination time, τ_{REC}. Figure 13 shows the temperature-dependent recombination rate ($1/\tau_{REC}$) assuming $T_i = T_e$ and a typical C-Mod density of 10^{20} m^{-3}. Insufficient experimental data are present to quantitatively derive the diffusivity due to the necessity of including the charge-exchange process, but for the few hundred eV temperatures present in $0.8 < r/a < 1.0$ in C-Mod Ohmic plasmas, $\tau_{REC} \sim$1 ms should be expected.

These estimates show that $\tau_\perp \sim \tau_\parallel$ is indeed a possibility in these C-Mod regimes. Together with the phenomenology of being correlated to a suspected change in turbulence regime and the parametric scaling shown in Section 4 that disagrees with neoclassical theory, a range of evidence supports the hypothesis that this asymmetry is sustained by turbulent transport mechanisms and

thus should be classified as non-neoclassical or anomalous. It is also worth noting that even if the C-Mod argon asymmetry is conclusively demonstrated to be driven by strong radial transport, this does not disprove or invalidate prior work [5][6] that showed a neoclassical up/down asymmetry. In many cases, these were observed with lower-Z impurities such as carbon, where the parallel diffusion time is smaller. Also, prior work has observed either broadband soft x-ray emission or line-emission from resonance transitions which are more characteristic of the local equilibrium. Conversely, this argues that observing discrete line emission dominated by recombination of high-Z impurities could lead to a new technique to study anomalous radial particle transport.

6 Summary

Observations of up/down asymmetries in argon soft x-ray emission have been observed to be in disagreement with neoclassical parallel impurity transport theory. The recently deployment of an advanced x-ray imaging crystal spectrometer has enabled previous C-Mod studies to be expanded to include a wider $\bar{n}_e$, I_p and B_T operating space in Ohmic plasmas. Measurements show a threshold behavior where argon emission for $0.8 < r/a < 1.0$ transitions from being nominally flux-surface symmetric to strongly up/down asymmetric with $\tilde{n}_z/\langle n_z \rangle$ of order unity. This occurs over a narrow operating range, $3.5 < B_t \bar{n}_e / I_p < 4.0$, at densities just below where the toroidal rotation reverses direction, a process linked to the transition between the linear and saturated Ohmic confinement regimes. This soft x-ray emission, originating from recombination from core Ar^{17+}, is indicative of strong cross-field transport and estimates of the parallel equilibration time on the order of 1 ms may not be sufficient to symmetrize any poloidally localized sources from turbulent transport.

7 Acknowledgments

This work supported by US DoE contracts DE-FC02-99ER54512 and in part by an appointment to the US DOE Fusion Energy Postdoctoral Research Program administered by ORISE. The authors would like to thank the PSFC staff for expert operation of the tokamak and C. Fenzi and D. Brower for useful discussions of their work.

A H-like Ar Continuity Equation for Edge Plasma

Estimates of argon transport can be used to show that the $\tilde{n}/\langle n_z \rangle \sim 1$ up/down asymmetry occurs in regions of the plasma where $\tau_\perp$ and $\tau_\parallel$ become the same order of magnitude. In order to calculate the radial transport time scale from observed emissivity profiles, the continuity equation for H-like Ar is simplified for use in the cold outer regions where the asymmetry is observed. The full continuity equation includes ionization and recombination to and from neighboring charge states,

$$\frac{\partial n_H}{\partial t} + \nabla \cdot \vec{\Gamma}_H = n_e \left[I_{He} n_{He} - (R_H n_H + I_H n_H) + R_f n_f \right] + n_0 \left(C_f n_f - C_H n_H \right) \tag{8}$$

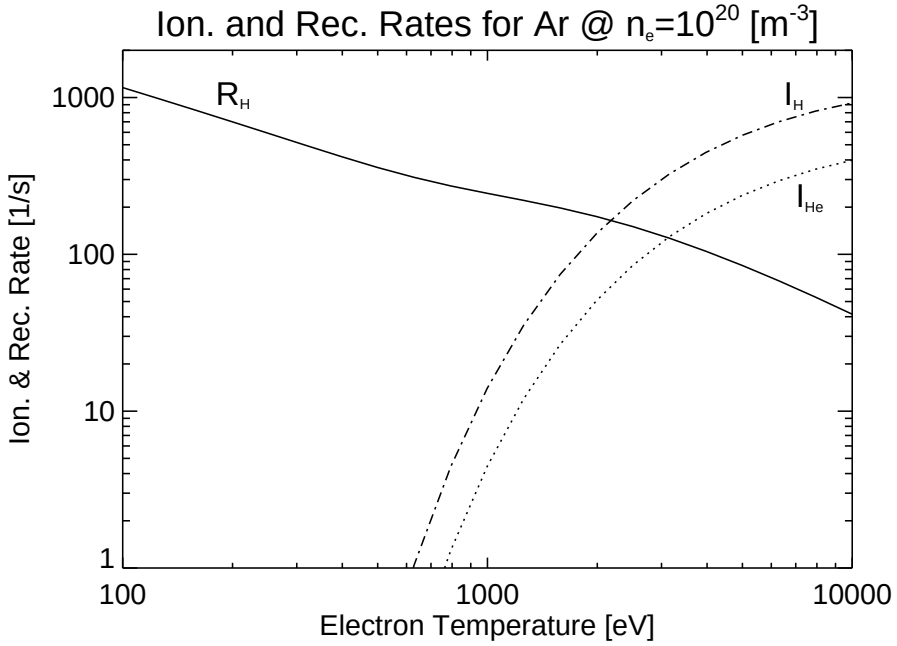

Figure 14: Ionization and recombination rates into (I_{He}) and out of (R_H, I_H) the H-like argon charge state for $n_e = 10^{20}$ m^{-3}

where the subscript f refers to the density of fully-stripped argon, H to hydrogen-like argon, and He to helium-like argon. The isoelectronic subscripts are used for clarity, but this equation can be generalized to any charge state of any ion. The ionization, I, and recombination, R, rates are known functions of electron temperature, while n_0 is the neutral density and C refers to the charge-exchange recombination rate. The time derivative is eliminated by observing the steady-state, and effects from fully-stripped argon, n_f, can be avoided by limiting the core T_e to prevent its production. In the outer layer of the plasma where the $\tilde{n}_z/\langle n_z \rangle$ starts to rise toward unity, ionization processes begin to turn off due to the low temperatures, and recombination rises as shown in Figure 14 for R_H, I_H and I_{He}. These rates are plotted in units of 1/s, assuming a local electron density of 10^{20} m^{-3}, and indicate that timescales of $\sim$1 ms, on order of the parallel transport time scale, are possible.

For $T_e < 1$ keV, the strong loss term from the H-like charge state allows the continuity equation to be approximated by

$$\nabla \cdot \vec{\Gamma}_H = -n_H \left(n_e R_H + n_0 C_H \right) \tag{9}$$

describing the change in the radial flux due to recombination. The measured z-line emissivity can be used to estimate n_H,

$$\varepsilon_z = n_H \left(n_e L_R \left(T_e \right) + n_0 L_C \left(T_i \right) \right) \tag{10}$$

where L_R is known from atomic physics modeling and n_e, T_e, and T_i are known. Measurements of neutral density, n_0, and atomic physics data for excitation via charge-exchange, L_C, are currently unavailable for these plasmas.

Figure 13 shows the relative strength of both R_H and C_H against temperature ($T_e = T_i$ assumed), for various neutral density fractions. The electron recombination term likely represents a lower limit,

with $n_0/n_e \sim 10^{-3}$ to 10^{-4} being reasonable estimates for the neutral density so close to the edge of the plasma. More data are required to quantitatively estimate the perpendicular transport time scale from (9), but there is a reasonable expectation that H-like Ar recombination times are below 1 ms at large minor radii. In order to have a flat z-line emissivity profile, as shown in Figure 7, $\tau_\perp \ll \tau_{REC}$ in order to transport H-like argon across the field before it has a chance to recombine.

References

[1] P. Smeulders. *Nucl. Fusion*, 26:267, 1986.

[2] H. Chen *et al*. *Phys. Plasmas*, 7:4567, 2000.

[3] L.C. Ingesson *et al*. *Plasma Phys. Control. Fusion*, 42:161, 2000.

[4] M.L. Reinke *et al*. *Plasma Phys. Control. Fusion*, 54:045004, 2012.

[5] K. Brau, S. Suckewer and S.K. Wong. *Nucl. Fusion*, 23:1657, 1983.

[6] W. Feneberg *et al*. Technical Report JET-R(86)07, JET Joint Undertaking, 1986.

[7] K.D. Marr *et al*. *Plasma Phys. and Control. Fusion*, 52:055010, 2010.

[8] T. Pütterich *et al*. *Nucl. Fusion*, 52:083013, 2012.

[9] P. Helander. *Phys. Plasmas*, 5:3999, 1998.

[10] S. Moradi *et al*. *Plasma Phys. Control. Fusion*, 53:115008, 2011.

[11] M.L. Reinke *et al*. *Rev. Sci. Instrum.*, 83:113504, 2012.

[12] M.L. Reinke. *Experimental tests of parallel impurity transport theory in tokamak plasmas*. PhD thesis, Massachusetts Inst. of Tech., 2011.

[13] J.E. Rice *et al*. *Nucl. Fusion*, 37:241, 1997.

[14] A. Ince-Cushman *et al*. *Rev. Sci. Instrum.*, 79:10E302, 2008.

[15] A. Bortolon *et al*. *Phys. Rev. Lett.*, 97:235003, 2006.

[16] J.E. Rice *et al*. *Nucl. Fusion*, 51:083005, 2011.

[17] J.E. Rice *et al*. *Phys. Plasmas*, 19:056106, 2012.

[18] C. Angioni *et al*. *Phys. Rev. Lett.*, 107:215003, 2011.

[19] J.E. Rice *et al*. *Phys. Rev. A*, 35:3033, 1987.

[20] S. Suckewer *et al*. Technical Report PPPL-1430, Princeton Plasma Physics Lab, 1978.

[21] D. Brower *et al*. *Phys. Rev. Lett*, 54:689, 1985.

[22] C. Fenzi *et al*. *Plasma Phys. Control. Fusion*, 41:1043, 1999.

[23] C. Fenzi *et al*. *Nucl. Fusion*, 40:1621, 2000.

[24] K.W. Wenzel. *Measurements on injected impurity transport in TEXT (Texas Experimental Tokamak) using multiply filtered soft x-ray detectors*. PhD thesis, Massachusettes Inst. of Tech., 1990.

[25] S.P. Regan. *Soft X-ray spectroscopy on the Phaedrus-T tokamak*. PhD thesis, Johns Hopkins Univerisity, 1996.

[26] R. Durst. *Nucl. Fusion*, 32:2238, 1992.

[27] J.L. Terry *et al*. *Phys. Rev. Lett.*, 39:1615, 1977.

[28] I. Condrea *et al*. *Plasma Phys. Control. Fusion*, 43:71, 2001.

[29] M.L. Reinke *et al*. *submitted to Phys. Plasmas*, 2012.

[30] J.E. Rice *et al*. *Rev. Sci. Instrum.*, 61:2753, 1990.

[31] T. Fülöp and P. Helander. *Phys. Plasmas*, 8:3305, 2001.

[32] M. Landreman, T. Fülöp and D. Guszejnov. *Phys. Plasmas*, 18:092507, 2011.

[33] N.P. Basse *et al*. *Fusion Sci. Tech.*, 51:476, 2007.

[34] A.H. Gabriel . *Mon. Not. R. Astr. Soc.*, 160:99, 1972.

[35] M.F. Gu *et al*. *Astrophys. J*, 582:1241, 2003.

[36] O. Marchuk *et al*. *J. Phys. B: At. Mol. Opt. Phys.*, 40:4403, 2007.

[37] B. Lipschultz *et al*. *Plasma Phys. Control. Fusion*, 44:733, 2002.

[38] J.E. Rice *et al*. *accepted in Nucl. Fusion*, 2012.

[39] P.H. Diamond *et al*. *Plasma Phys. Control. Fusion*, 47:R35, 2005.

[40] P. Helander and D.J. Sigmar. *Collisonal Trasnport in Magnetized Plasmas*. Cambridge University Press, 2002.

[41] A. Kramer-Flecken *et al*. *Phys. Rev. Lett.*, 97:045006, 2006.

[42] G.R. McKee *et al*. *Phys. Plasmas*, 10:1712, 2003.

[43] T. Ido *et al*. *Plasma Phys. Control. Fusion*, 48:S41, 2006.

[44] S. Braun *et al*. *Plasma Phys. Control. Fusion*, 51:065011, 2009.

[45] M. Sasaki *et al*. *Plasma and Fusion Research*, 3:S1017, 2008.

[46] W. Guo *et al*. *Phys. Plasmas*, 17:112510, 2010.